A DILATANCY-DAMAGE MODEL CONSIDERING TEMPERATURE EFFECT FOR ROCK SALT FROM AN UNLOADING PATH

by

Zhongguang SUN[a,b,c], Jinyang FAN[a,b*], Fei WU[a,b*], and Jie CHEN[a,b],

[a] State Key Laboratory for the Coal Mine Disaster Dynamics and Controls, Chongqing University, Chongqing, China
[b] College of Resources and Environmental Science, Chongqing University, Chongqing, China
[c] State Key Laboratory of Gas Disaster Detecting China Coal Technology and Engineering Group, Chongqing, China

Original scientific paper
https://doi.org/10.2298/TSCI180823223C

Investigating the dilatancy of host rock during stress re-distribution is of great significance for underground engineering, especially underground salt cavern storages. To formulate the dilatancy variation, some measurements were conducted via unloading tests with ever-reduced confining pressure and constant axial pressure. The results demonstrated that the initial confining pressure had little influence on the dilatancy of rock salt. A larger axis pressure can promote the dilatancy of rock salt. A higher temperature would accelerate the dilatancy rate and augment the total volumetric expansion. A dilatancy-damage model was established by using theoretical deduction and numerical fitting, which showed a good agreement with test data.

Key words: *rock salt, dilatancy-damage, unloading confining pressure, temperature*

Introduction

Rock salt, due to its low permeability and excellent creep performance, is recognized as one of the most effective and stable storage medium for natural gas and oil*, etc.* [1-3]. Owing to the extensive distribution and relatively low cost, underground salt caverns (USC) are widely developed and used throughout the world. So far, more than 60 USC in Europe have been constructed with the working gas capacity exceeding $500 \cdot 10^8$ m^3. Meanwhile, by the end of 2012, there were 40 salt cavern gas storages in America [4-6]. In order to ensure the availability of energy supply, the Chinese government is actively organizing the research and construction of underground salt storages. One of the main challenges is to analyze the stability and isolation (anti-permeability) properties of the USC. Dilatancy behavior is a good indicator which can simultaneously reflects the damage and permeability of rock salt [7, 8].

In the underground geo-engineering field, a large number of studies on dilatancy have been conducted. Hunsche *et al*. [9] proposed an elasto-viscoplastic constitutive model describing dilatancy, healing, damage, failure, and deformation of rock salt. Tan *et al*. [10] through triaxial compression tests, experimentally observed and numerically simulated granite's permeability evolution during its progressive failure. Alkan *et al*. [11] reported the results of an experimental investigation on the dilatancy behavior and its influence on USC, implying that the main reason for the isolation failure of salt gas storage is the generation and development

* Corresponding author, e-mail: Jingyang.f@cqu.edu.cn; wufei361@cqu.edu.cn

of dilatancy in excavated disturbed zones along the boundary of the cavity and rock. Actually, in the process of constructing and operating salt cavern gas storages, the surrounding rock usually experiences an unloading stress path. Most of the aforementioned calculation models and methods were based on conventional compression tests, which because of certain limitations could not be used directly in analyzing the stability and isolation properties of USC. This work focuses on the dilatancy characteristics of rock salt for different factors (confining pressure, axis pressure and temperature) in an unloading path.

Test conditions and test scheme

The rock salt samples were collected from the Khewra salt mine, Pakistan and shaped into cylinders (50 mm × 100 mm). The initial wave velocity of rock salt was measured using ultrasonic wave technology, to examine the similarity among the samples. After that, the samples with no cracks and similar velocity were tested using the MTS815.03 Electro Hydraulic Servo Rock Experiment System.

The tests were performed in two steps:

– preparation/loading phase: increase the confining pressure and the axis pressure to designed values with a loading rate of 0.02 MPa/s and
– unloading phase: keep the axis pressure constant and decrease the confining pressure to 0 at a constant speed.

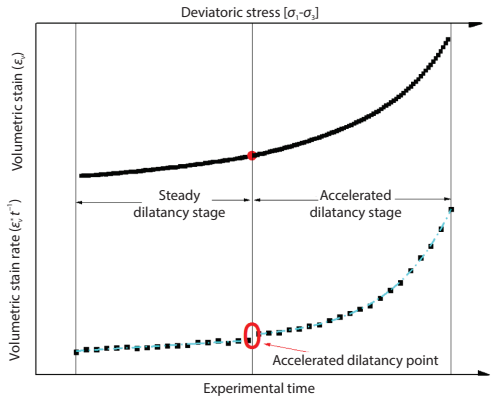

Figure 1. Representative deviatoric stress/time-volumetric strain curves

Test results and discussions

The segmentation characteristics of dilatancy

A representative curve of the volumetric strain-deviatoric stress from the unloading tests is shown in fig. 1. The point where the volumetric dilatancy rate exceeds 10% of the initial dilatancy rate is defined as the dividing point (accelerated dilatancy point – ADP) of the two-stages (the steady dilatancy stage and the accelerated dilatancy stage). Its corresponding stress is named after the critical deviatoric stress, σ_c. The difference in two-stages is clear: steady dilatancy stage – the original compacted pore and crack in the rock will re-open as the confining pressure gradually reduces and accelerated dilatancy stage – the interspaces and microcracks in the sample completely re-open, the stress concentration around the defects reaches the failure limitation, more and more original cracks propagate and new cracks initiate.

Effect of deviatoric stress

The ADP are marked on the curves from the tests under different initial confining pressures including 10 MPa, 15 MPa, and 20 MPa in fig. 2(a). The results show that the volumetric strain increases slowly in the first stage, then dramatically increases in the second stage. It is important to note that the critical confining pressures are almost the same, implying that the initial confining pressure has seldom influence on the σ_c but could enhance volumetric expansion.

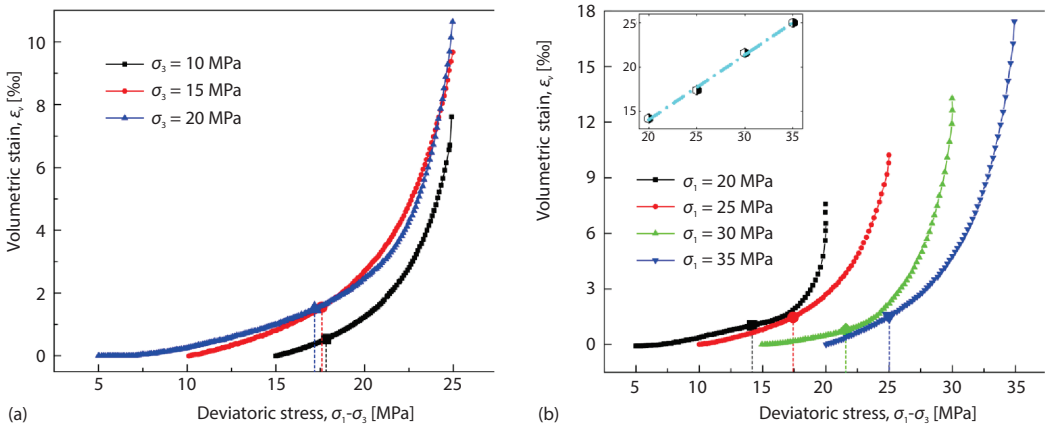

Figure 2. Deviatoric stress-volumetric strain curves of the specimens; (a) different values of initial confining stress, (b) different values of axial pressure

The curves of deviatoric stress *vs.* volumetric strain for rock salt under different axial pressures are shown in fig. 2(b). It is clear that the axial pressure affects the dilatancy more strongly. When the axial pressure is 20 MPa, 25 MPa, 30 MPa, and 35 MPa, the σ_c is 14.2 MPa, 17.4 MPa, 21.6 MPa, and 25 MPa, respectively. The critical stress is linearly dependent on the axial pressure, see inset in fig. 2(b).

Effect of temperature

Results for the samples tested at 15 °C, 30 °C, 45 °C, and 60 °C, as shown in fig. 3. As we can see, a higher temperature would not only lead to an advanced ADP but also to a higher dilatancy rate and amplitude. To further the investigation on unloading dilatancy, we measured the wave velocity after testing rock salt samples and calculated their damage value through eq. (1).

$$D = 1 - \left(\frac{v'}{v_0}\right)^2 \tag{1}$$

where D is the damage, v' and v_0 represent the wave velocity after the tests and the initial wave velocity before the tests, respectively. It can be found that the damage of rock salt increases as the temperature increases. Many scholars explained the effect of temperature via the ductility performance and plasticity performance of materials [12, 13]. A higher temperature could enhance the creep.

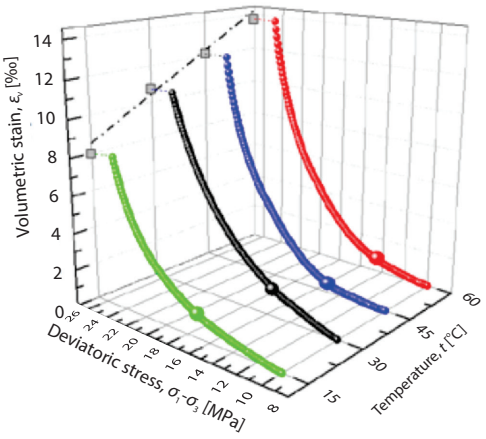

Figure 3. Deviatoric stress-volumetric strain curves for specimens at different temperatures

Dilatancy-damage model

Establishment of dilatancy-damage model

During the unloading process in tests, the rocks experienced axial compression and radial expansion. It could be noticed that the deformation was uniform, inerratic, and no macroscopic crack occurred. In addition, it can be assumed that the deformation direction is consistent

with the outward normal direction of the yield surface. The thermodynamic intrinsic dissipation rate inequality [13]:

$$\frac{V\sigma_{ij}}{m}\dot{\varepsilon}_{ij}^{p} - R\dot{p} - Y\dot{D} \geq 0 \tag{2a}$$

And

$$\begin{cases} \dot{\varepsilon}_{ij}^{p} = \lambda \dfrac{\partial F_p}{\partial (V\sigma_{ij}/m)} \\ \dot{p} = \lambda \dfrac{\partial F_p}{\partial R} \\ \dot{D} = \lambda \dfrac{\partial F_p}{\partial Y} \end{cases} \tag{2b}$$

where F_p is the plastic potential function, V – the volume of the sample, m – the mass of the sample, R – the increment of the yield surface, and Y – the damage strain energy release rate.

Assuming that damage is only relevant with the second invariant of deviatoric stress, according to the Von Mises criterion, $\sigma_n = \sigma_{kk}/3$, we have:

$$F_p = \left(\frac{V\sigma_{ij}}{m}\dot{\varepsilon}_{ij}^{p}, R, Y\right) = \sigma_{ij} - (R_0 + R) - Yg\left(\frac{V\sigma_n}{m}\right) \tag{3}$$

Substituting eq. (3) into eq. (2b), and calculating its partial derivative, then:

$$\begin{cases} \dot{e}^{p} = \dfrac{3\lambda}{2\sigma_p} S \\ \dot{\varepsilon}_{V}^{p} = \dfrac{\lambda Y}{3} g'\left(\dfrac{V\sigma_n}{m}\right) \\ \dot{p} = \lambda \\ \dot{D} = \lambda g\left(\dfrac{V\sigma_m}{m}\right) \end{cases} \tag{4}$$

where $\dot{e}^{p}$ is the plastic deviatoric stress tensor, σ_p – the plastic deviatoric stress, and $\dot{\varepsilon}_{V}^{p}$ – the plastic volumetric strain tensor.

If the damage variable is directly related to the volume, $\dot{D} = \mathrm{D}'(V)\dot{V}$ where $\dot{V}$ is the first-order derivative. Based on the mass conservation law, we have:

$$g\left(\frac{V\sigma_n}{m}\right) = c\exp\frac{V\sigma_n}{m\sigma} \tag{5}$$

where c is the integral constant.

Therefore:

$$D = \ln\left(1 + \frac{V-m}{mf_0}\right) \tag{6}$$

Then eq. (5) can be simplified:

$$D = \ln\left(1 + \frac{\varepsilon_V}{1-a}\right) \tag{7}$$

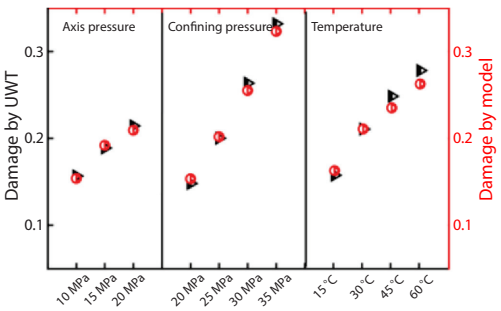

Figure 4. Values of damage obtained by two different methods

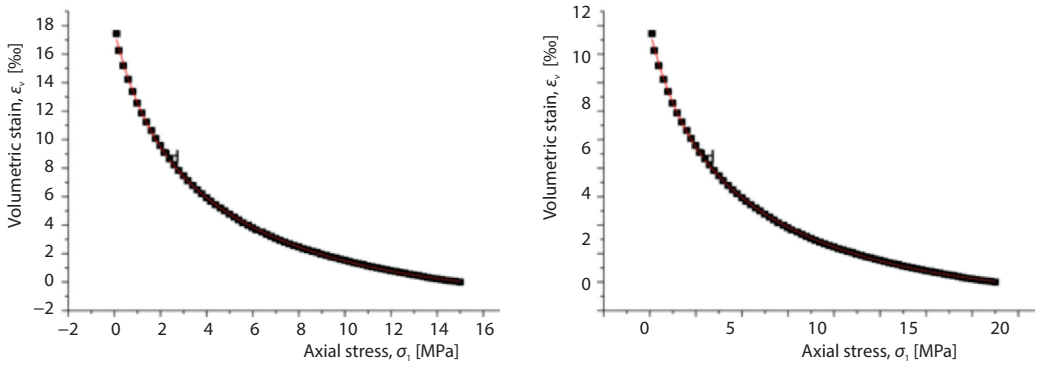

Figure 5. Test curves and regression curves of the stress *vs.* the volumetric strain

where $(1 - f_0)m/V_0 = a$, f_0 is the initial void ratio of the sample, V_0 – the initial volume. The calculated damage using eq. (7) shows a good agreement with the damage measured by UWT and eq. (1), fig. 4. Therefore, it is reasonable to calculate the dilatancy-damage of rock salt using eq. (7).

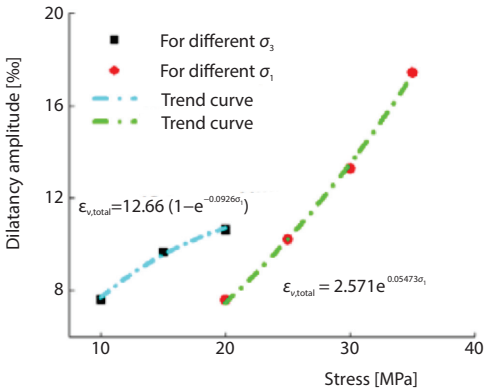

Figure 6. Dilatancy amplitude from tests on the confining pressure group and the axial pressure group

Extended dilatancy damage model

– Relationship between deviatoric stress and volumetric strain

The fitting results show that deviatoric stress is an exponential function of volumetric strain during the whole process of unloading the cinfining pressure. Here we present one representative case for the axial stress (35 MPa) and the confining stress (20 MPa), as shown in fig. 5. Besides, fig. 6 shows that the dilatancy increment induced by the axial stress is larger than that induced by the confining stress. Thus, it is necessary to introduce two groups of undetermined coefficients (a_1, a_3, b_1, b_3) to distinguish the different weights. The relationship is:

$$\varepsilon_V = \varepsilon_{V0} + A_1 \exp(a_1\sigma_1 - a_3\sigma_3) + B_1 \exp(b_1\sigma_1 - b_3\sigma_3) \tag{8}$$

where σ_1 is the first principal stress, σ_3 – the third principal stress, ε_V – the volumetric strain while, ε_{V0} – the initial tiny compression volumetric strain. The values of the main parameters are listed in tab. 1.

– In fig. 3, the maximum volumetric strain of each curve was projected to the left co-ordinate plane and showed an approximate linear growth. If we define a basic test, the temperature factor, k_T, can be defined and imported to amend the eq. (8).

$$\varepsilon_V(T) = \varepsilon_V(T_0)\left[\left(\frac{\varepsilon_V(T) - \varepsilon_V(T_0)}{\varepsilon_V(T_0)}\right)\frac{1}{T - T_0}(T - T_0) + 1\right] = \varepsilon_V(T_0)[k_T(T - T_0) + 1] \tag{9}$$

and

$$D = \ln\left(1+\left[\varepsilon_{V0} + A_1 e^{a_1\sigma_1 - a_3\sigma_3} + B_1 e^{b_1\sigma_1 - b_3\sigma_3}\right]\left[k_T(T-T_0)+1\right]\frac{1}{1-a}\right) \tag{10}$$

where T, T_0, $\varepsilon_V(T)$, and $\varepsilon_V(T_0)$ represent the real-time temperature, the initial temperature of the basic test, the real-time volumetric strain and the volumetric strain of the basic test. Substituting eq. (9) into eq. (7), we can obtain the dilatancy-damage model given by eq. (10) as a function of stress and temperature.

Table 1. Values of main parameters

Parameters	Values	Remarks	Parameters	Values	Remarks
a	0.9553	–	b_1	0.0665	–
ε_{V0}	–0.6959	$\cdot 10^{-3}$	b_3	0.7449	–
A_1	1.8636	–	v_0	0.005	[kNs^{-1}]
a_1	0.0551	–	T_0	15	[°C]
a_3	0.1667	–	k_T	0.2152	–
B_1	0.5792	–			

It is worth noting that these laws are obtained within the scope of the tests. If the stress condition changes, the temperature factor, k_T, may change concomitantly. For this model, it is easy to achieve the targeted values of involved parameters by the regression of pre-test data.

In China, the general building depth of USC ranges from 600-1800 m. The operation gas pressure ranges from 5-18 MPa. Accordingly, the vertical pressure and the horizontal pressure of surrounding rock vary from 15-45 MPa and from 5-20 MPa, respectively. The experimental scope in the unloading tests can almost cover practical situations. Therefore, the dilatancy-damage model is able to predict the dilatancy deformation and damage evolution of the surrounding rock salt, as well as the variation of porosity and permeability if combined with the result by Alkan *et al*. [11].

Conclusion

In the present work, the dilatancy characteristics and mechanisms of rock salt under the action of the unloading confining pressure were studied. It was found that.

- Initial confining pressure has little influence on the dilatancy for rock salt. The growth of the axial pressure can promote the dilatancy and move the accelerated dilatancy point forward. Meanwhile, the critical deviatoric stress linearly increases with the axial pressure.
- As the temperature increases, the accelerated dilatancy point of the rock salt will advance by extending the accelerated dilatancy stage. Besides, the dilatancy rate and amplitude will be enhanced too.
- The dilatancy-damage model based on the stress and the temperature was established by theoretical derivation and numerical fitting. There is a good correlation between test results and the model. The scope of the experimental factors can cover the current situation of USC and can be helpful for predicting the dilatancy deformation and damage evolution.

Acknowledgment

This work was supported by the National Natural Science Fund (No. 51834003, 41672292, 51704044), China Postdoctoral Science Foundation (2018M633318), Chongqing Postdoctoral Innovation Program (CQBX201802), the Fundamental Research Funds for the Central Universities (No. 2018CDQYZH0018), which are all greatly appreciated.

Nomenclature

A_1 – regression coefficients, [–]
B_1 – regression coefficients, [m^3]
f_0 – the initial void ratio, [%]
k_T – temperature factor, [–]
m – rock mass, [kg]
T – absolute temperature, [K]
V_0 – initial volume, [m^3]
v_c – speed, [ms^{-1}]

Greek symbols

ε_V – volumetric strain, [m^3]
ε_{V0} – initial compression volumetric strain, [–]
σ_1 – axial stress, [MPa]
σ_3 – lateral stress, [MPa]

References

[1] Deng, J. Q., *et al.*, Time-Dependent Behaviour and Stability Evaluation of Gas Storage Caverns in Salt Rock Based on Deformation Reinforcement Theory, *Tunnelling and Underground Space Technology*, *42* (2014), May, pp. 277-292
[2] Fan, J., *et al.*, Discontinuous Cyclic Loading Test with Acoustic Emssion Monitoring, *International Journal of Fatigue*, *94* (2017), Part 1, pp. 140-144
[3] Yang, C., *et al*., Daemen, Feasibility Analysis of Using Abandoned Salt Caverns for Large-Scale Underground Energy Storage in China, *Applied Energy*, *137* (2015), pp. 467-481
[4] Moghadam, S. N., *et al.*, Parametric Assessment of Salt Cavern Performance Using a Creep Model Describing Dilatancy and Failure, *International Journal of Rock Mechanics and Mining Sciences*, *79* (2015), Oct., pp. 250-267
[5] Jiang, D., *et al.*, A Mechanism of Fatigue in Salt Under Discontinuous Cycle Loading, *International Journal of Rock Mechanics and Mining Sciences*, *86* (2016), July, pp. 255-260
[6] Fan, J., *et al.*, Thermodynamic and Applicability Analysis of a Hybrid CAES System Using Abandoned Coal Mine in China, *Energy*, *157* (2018), Aug., pp. 31-44
[7] Alkan, H., *et al.*, Percolation Model for Dilatancy-Induced Permeability of the Excavation Damaged Zone in Rock Salt, *International Journal of Rock Mechanics and Mining Sciences*, *46* (2009), 4, pp. 716-724
[8] Wu, F., *et al.*, A Non-Linear Creep Damage Model for Salt Rock, *International Journal of Damage Mechanics*, *28* (2018), 5, pp. 758-771
[9] Hunsche, U., *et al.*, Rock Salt – The Mechanical Properties of the Host Rock Material for a Radioactive Waste Repository, *Engineering Geology*, *52* (1999), 3-4, pp. 271-291
[10] Tan, X., *et al.*, Experimental and Numerical Study on Evolution of Biot's Coefficient During Failure Process for Brittle Rocks, *Rock Mechanics and Rock Engineering*, *48* (2014), 3, pp. 1289-1296
[11] Alkan, H., *et al.*, Rock Salt Dilatancy Boundary from Combined Acoustic Emission and Triaxial Compression Tests, *International Journal of Rock Mechanics and Mining Sciences*, *44* (2007), 1, pp. 108-119
[12] Fan, J., *et al.*, Discontinuous Fatigue of Salt Rock with Low-Stress Intervals, *International Journal of Rock Mechanics and Mining Sciences*, *115* (2019), pp. 77-86
[13] Zhang, G., *et al*., Daemen, Stability and Tightness Evaluation of Bedded rock Salt Formations for Underground Gas/Oil Storage, *Acta Geotechnica*, *9* (2013), pp. 161-179

Paper submitted: August 23, 2018
Paper revised: November 19, 2018
Paper accepted: February 11, 2019